



Temperature induced formation of particle coated non-spherical droplets

Junjun Tan, Mei Zhang, Jun Wang, Jian Xu, Dejun Sun*

Key Laboratory of Colloid and Interface Chemistry, Shandong University, Ministry of Education, Jinan, 250100 Shandong, PR China

ARTICLE INFO

Article history:

Received 30 November 2010

Accepted 18 March 2011

Available online 24 March 2011

Keywords:

Pickering emulsion

Non-spherical droplets

Partial coalescence

Temperature

Mg(OH)₂ nanoparticles

ABSTRACT

Herein we offer a simple method to produce non-spherical emulsion droplets stabilized by freshly formed Mg(OH)₂ nanoparticles (MPs). The non-spherical degree of droplets as a function of experiment conditions was investigated and the origins of the presence of non-spherical droplets were discussed. The results of optical microscope images show that stable spherical droplets can be fused into non-spherical at given aging temperature. It is also recognized that particle concentration, oil/water ratio and aging time significantly affect droplet fusion and excess particles that are not adsorbed on the oil/water interface are helpful in restraining droplet fusion. Based on the TEM, XRD and Fluorescence confocal microscopy results, the origins of droplet fusion are inferred from the presence of vacant holes in the particle layer. Because of Oswald ripening, particles on droplet surfaces grow larger than the freshly precipitated ones under a given aging temperature. The growth of particles results in the reduction of total cover area of particle layer and thus creates vacant holes in the particle layer which would cause partial coalescence of droplets once they collide. Thus, these findings can offer a simple alternative to obtain a large amount of non-spherical emulsion droplets but also can help the preparation of non-spherical colloid particles.

© 2011 Elsevier Inc. All rights reserved.

1. Introduction

Non-spherical particles, which are different from spherical particles in packing density and symmetry [1] are increasingly significant in tailoring the photonic properties of colloidal assemblies [2,3], controlling their assembly at fluid interfaces [4–6], and even creating complex particle structures [7,8]. Lots of efforts have been made to synthesize or fabricate non-spherical particles, including seeded emulsion polymerization [9,10], stretching particle-embedded polymer films [11], photolithography [12], microcontact printing [13], and the use of microfluidic devices to deform emulsion droplets [14–16]. But these methods are rather complicated and heavily rely on devices. Our attention has been focused on emulsion template method, which has been widely used as templates in the fabrication of spherical colloidal particles and relevant materials and structures [17–19] and is expected to be device-free; it is very interesting to investigate whether the method could be applied to produce non-spherical particles.

Generally, spherical shape is the most common morphology in emulsions and such a statement has been well supported by ample practical and theoretical evidences [20,21]. As the interface area should be minimized to a given volume because of the minimiza-

tion of surface energy, it is difficult to directly produce stable non-spherical emulsion droplets because of the unbalanced stress induced by non-spherical shape of droplets. To be specific, non-spherical emulsion droplets would soon recover to be spherical even if they can be formed temporarily.

Recently, it is recognized that particle-coated bubbles and droplets can keep being non-spherical because the outer particle shell can withstand the unequal stress of interfaces with unequal radii of curvature. Up to now, non-spherical structures have been obtained by squeezing particle-coated air bubbles [16] and oil droplets between glass slides and through a glass capillary [14] or elongating them in sheared particle-stabilized emulsions [15]. These findings suggest that droplets or bubbles can also be shaped into tailored anisotropic geometries [9,14–16,22–30]. Furthermore, these significant works offer us an effective method to produce non-spherical droplets. However, most of the findings reported are based on micro-fluidic technology. How to produce a large quantity of non-spherical droplets without any special device is still a challenge.

To date, systematic study on the preparation of non-spherical droplets induced by temperature has not yet been reported. Our previous work has demonstrated that in situ formed Mg(OH)₂ nanoparticles (MPs) are excellent emulsion stabilizers with pH switchability [31]. The objective of this report is to offer a simple method to generate non-spherical emulsion droplets stabilized by MPs by adjusting aging temperature.

* Corresponding author. Fax: +86 531 88365437.

E-mail address: djsun@sdu.edu.cn (D. Sun).

2. Experiments and methods

2.1. Materials

The deionized water was purified by ion exchange. The oil phase was liquid paraffin (Sinopharm Chemical Reagent Co., China) with purity greater than 99% ($d_{420} = 0.835\text{--}0.855$). The composition of liquid paraffin is mainly isoalkane and the main carbon number distribution measured with Agilent 6820 GC (Agilent Co., USA) is between 16 and 26. Magnesium chloride, Sodium hydroxide used here was chemical grade (Kemeng Chemical Reagent Co., China). Styrene (Sinopharm Chemical Reagent Co., China) was washed with 5% NaOH and dried over anhydrous MgSO_4 , and distilled under reduced pressure.

Crystalline magnesium hydroxide, the so-called Brucite belongs to the bivalent metal hydroxides group, whose crystal structure is a layered CdI_2 -type arrangement. Successive hexagonal Mg^{2+} ions layers and OH^- ions layers are stacked one upon another. The magnesium cation is sixfold coordinated by hydroxyl groups, thus forming $\text{Mg}(\text{OH})_6$ octahedra. Such a layered crystal structure is an advantage for platelet-shaped crystallization of the compound [32]. The density of crystalline magnesium hydroxide is 2.59 g/cm^3 . Crystalline magnesium hydroxide is hydrophilic with contact angle of 15° according to our previous reports [31].

2.2. Methods

2.2.1. Preparation of $\text{Mg}(\text{OH})_2$ suspensions

In a typical experiment, 2 mL MgCl_2 (1 M) was added to 16 mL deionized water in a beaker. Then 4 mL NaOH (1 M) was poured into the beaker and kept being homogenized at 6000 rpm for 5 min (Shanghai Forerunner M&E Co., China). Then the solution was transferred to a sealed aging tank (steel outside, PTFE inside) and treated at different aging temperatures for 16 h. After that, the white sediment was filtrated and dried under vacuum at 25°C for 24 h. The obtained powder was characterized by X-ray diffraction. The XRD instrument was a $D/\text{max-}\gamma B$ diffractometer with $\text{Cu K}\alpha$ radiation. Data were collected over the 2θ ranging from 2° to 70° . A JEM-100CX II electron microscope was used to observe the morphology of MPs.

2.2.2. Preparation, stability and characterization of emulsions

Typically, 20.0 mL liquid paraffin and 20.0 mL aqueous dispersion at pH 10.5 values with different initial MgCl_2 concentration were placed in a glass vessel (inner volume 100 mL) at room temperature and then homogenized at 6000 rpm for 2 min with a homogenizer (Shanghai Forerunner M&E Co., China). Immediately after homogenization, the emulsion was put into a sealed aging tank for a period of time at a specific temperature. The emulsion type was inferred by observing whether a drop of the emulsion can be dispersed when it was added to a small volume of water or oil. The stability of emulsions at 20°C was assessed by monitoring the movement of the oil–emulsion and water–emulsion interfaces. For water-continuous emulsions, the position of the oil–emulsion interface was used as an indicator of coalescence. The pH of the dispersion was monitored by a Corning model 440 benchtop pH meter. Small samples of emulsion/dispersion were placed in a glass slide and viewed with an Axioskop 40 optical microscope (ZEISS, Germany). Photographs of vials containing emulsions were taken with a Canon PowerShot S5 IS digital camera. The emulsion droplets were diluted in water at the same pH and NaCl concentration as those in the original aqueous dispersion and circulated through the dispersion unit. All images were processed with Adobe Photoshop software CS2 edition. Non-spherical degree of emulsion droplets was measured using statistical meth-

od from three random microscope images (200 counts at least). A laser-induced confocal microscope (Olympus Fluoview 500, Japan) was used to investigate the adsorption of MPs on the emulsion surface. The fluorescent probe was Rhodamine B, which is negatively charged in basic solution and has a maximum excitation wavelength at 543 nm. The MPs were labeled with Rhodamine B in the following procedures: a mass of Rhodamine B was added into 25 mL aqueous dispersion which contained 0.5 wt.% MPs. The concentration of Rhodamine B in the mixed aqueous dispersion was fixed at $1.0 \times 10^{-5} \text{ M}$. The prepared dispersions were stirred for 1 h to get adsorption equilibrium. Then emulsions stabilized by fluorescence-labeled particles were prepared and fluorescent images of emulsions were observed under microscope.

3. Results and discussion

For emulsion stabilized by colloidal particles, spherical shape is universal. Fig. 1 illustrates the shapes of emulsion droplets at different aging temperatures. At the temperature of 25°C nearly perfect spherical drops can be observed, even after being rested for more than a few weeks (Fig. 1a). This phenomenon would be attributed to the presence of particle layer on the droplet surface which can strongly resist coalescence [20]. However, when the aging temperature was kept above 80°C for 16 h, a certain number of spherical droplets would become non-spherical as shown in Fig. 1b. As the aging temperature keeps rising, the proportion of non-spherical droplets produced increases. Based on the observation, it is possible to produce large quantities of stable non-spherical emulsion droplets just through aging temperature regulation.

The works we have done in the following sections can help us to find out the conditions which facilitate the formation of non-spherical droplets. The effect of particle concentration, oil/water ratio, aging temperature and aging time on the non-spherical degree of droplets will be discussed as well. Unlike spherical droplets, it is difficult to define the geometry of non-spherical droplets, like the ones represented in Fig. 1. To qualitatively analyze the non-spherical degree of droplets, emulsions at different aging temperatures were investigated. Each droplet was treated with circumscribed rectangular in the images. Therefore, it is possible to introduce the ratio d defined as

$$d = \sum_n D_{\text{max}} / D_{\text{min}} \quad (n > 200)$$

where d was defined as a value to evaluate the non-spherical degree, D_{max} and D_{min} were defined as the longer side and the shorter side of a droplet respectively. When d is equal to 1, droplets are all spherical. When it is above 1, a certain number of non-spherical droplets begin to show up. 200 emulsion droplets from at least three random optical micrographs are used for statistic analysis. Also the releasing oil fraction, which is the ratio of releasing oil volume and total oil volume, is used to evaluate the level of oil released from droplets and it can help us to find out the relationship between emulsion stability and the proportion of non-spherical droplets.

The value of d as a function of particle concentration at different aging temperatures is represented in Fig. 2a. The variation of d could be divided into two stages. When the particle concentration is below 0.145 wt.%, the d drops sharply from its initial high point; above that particle concentration, the falling speed of d begins to slow down and approaches 1.0 when aging temperature is lower than 80°C . Therefore, raising aging temperatures is in favor of forming non-spherical droplets. The oil releasing fraction shows a similar tendency, it decreases along with the increase of particle concentration and increases with the rise of aging temperature. Based on the results, it is recognized that aging temperature is an important driving force for the formation of non-spherical drop-

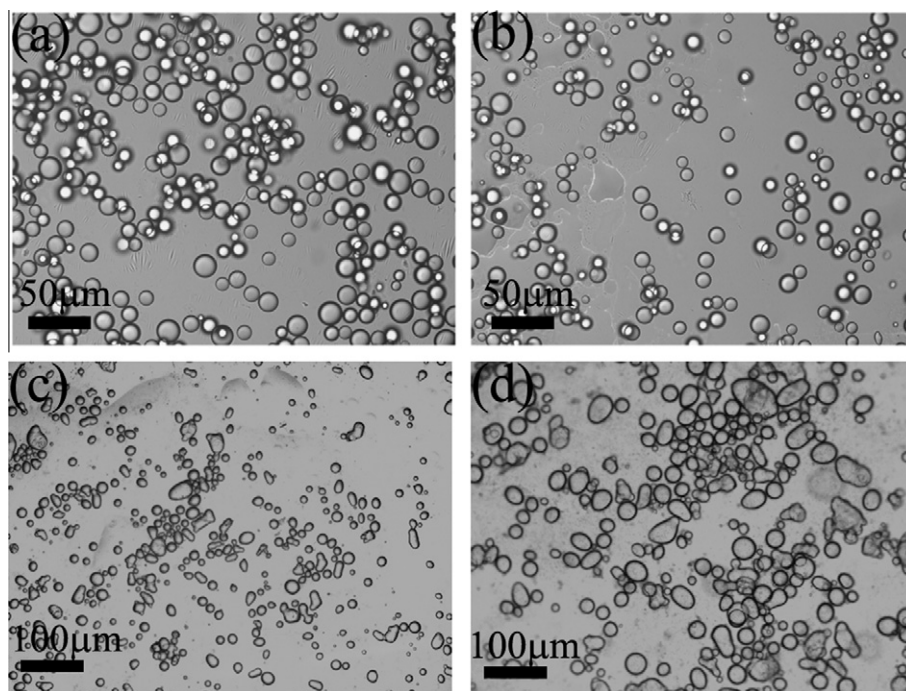


Fig. 1. Microscope pictures of emulsion droplets stabilized by MPs at the temperature of: 25 (a), 80 (b), 160 (c) and 200 °C (d) for 16 h. The scale bar is 200 μm .

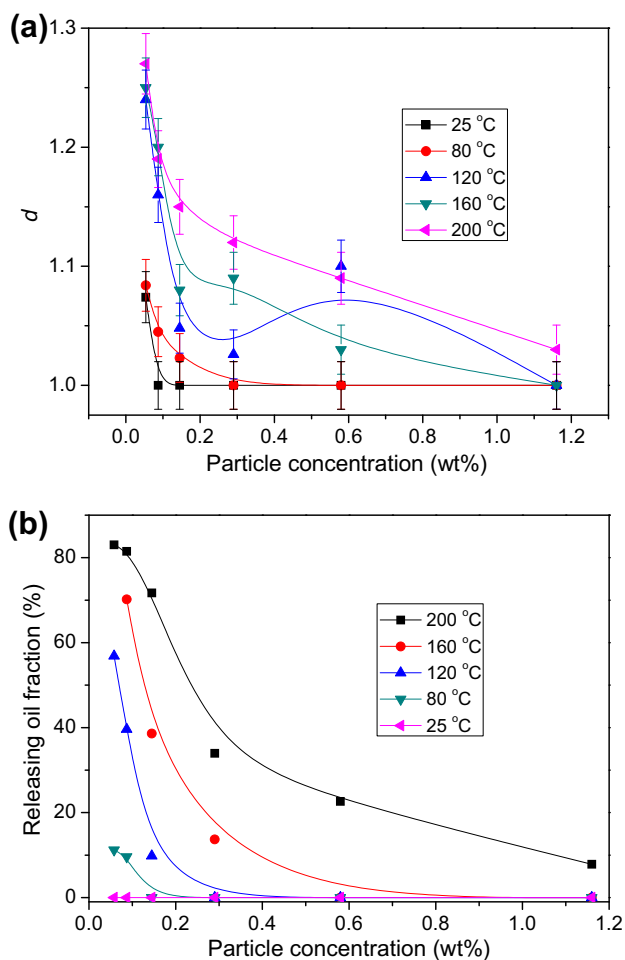


Fig. 2. Non-spherical degree of droplets (a) and releasing oil fraction of emulsions; (b) as a function of particle concentrations at different temperatures, the ratio of oil volume and water volume is 1.

lets. In summary, low particle concentration and high aging temperature are not the expected conditions for the production of non-spherical droplets because under these circumstances, though relatively high non-spherical degree could be got, the emulsion stability is decreased seriously as the oil phase released is high. Similarly, although the amount of oil phase released could be reduced to a great extent under high particle concentration and low aging temperature, the non-spherical degree of droplets would become low, so this cannot be taken as a proper condition either. So the practical conditions for non-spherical droplet production are particle concentration of 0.2–0.6 wt.% and aging temperature of 120–160 °C.

As discussed above, temperature and particle concentration play significant roles in the formation of non-spherical droplets. So if particle concentration works on the non-spherical degree of droplets, it is interesting to ask whether variation of oil/water ratio can affect the non-spherical degree of droplets as well. Therefore, shapes of droplets at different oil/water ratios were compared and the value of d as a function of the temperature and oil/water ratio is shown in Fig. 3a.

We can see that the d value shows a gradual increase and goes up to the peak when oil phase content is 12.5% which corresponds to the maximum non-spherical degree of droplets. From 12.5 to 37.5%, the d stays at a high value plateau, indicating that droplets at this oil–water ratio facilitate the formation of non-spherical droplets. Further increase of the oil phase content decreases the d value, suggesting that relatively high oil–water ratio of emulsion cannot offer any positive effect on the formation of non-spherical droplets. At the same time, oil releasing fraction is also represented in Fig. 3b. As can be seen from Fig. 3b, the oil releasing fraction is close to zero at the aging temperature of 25 °C. Further increase of the aging temperature separates oil releasing fraction into two parts, when oil content is below 30%, there is rarely any oil phase released and above that percentage oil phase released increases, suggesting that during the whole aging process, high oil/water ratio of emulsion presents a negative factor for the emulsion stability.

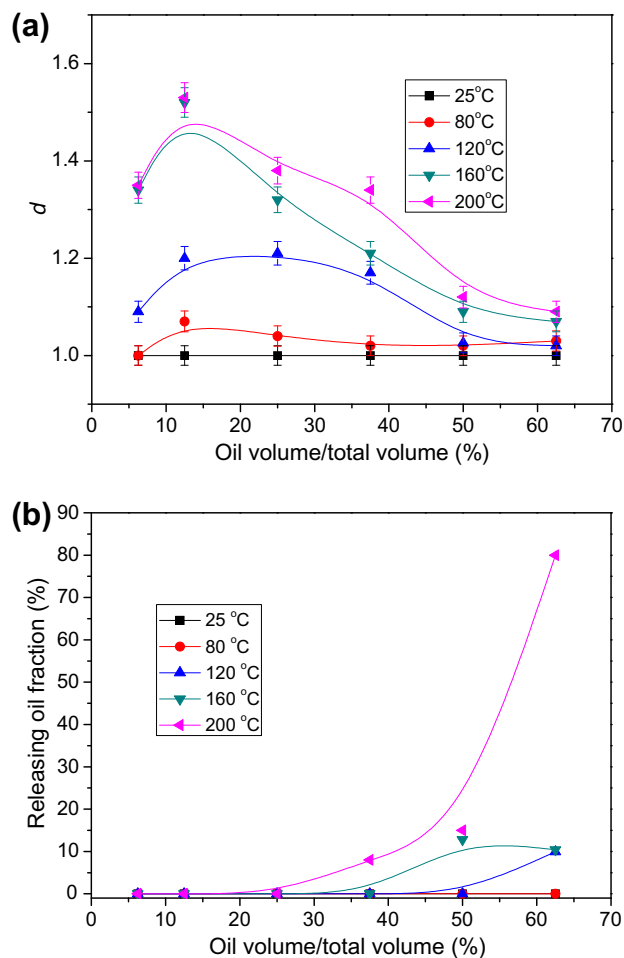


Fig. 3. Non-spherical degree of droplets (a) and releasing oil fraction of emulsions; (b) as a function of oil/water ratio at different temperatures. The particle concentration is 0.29 wt.%.

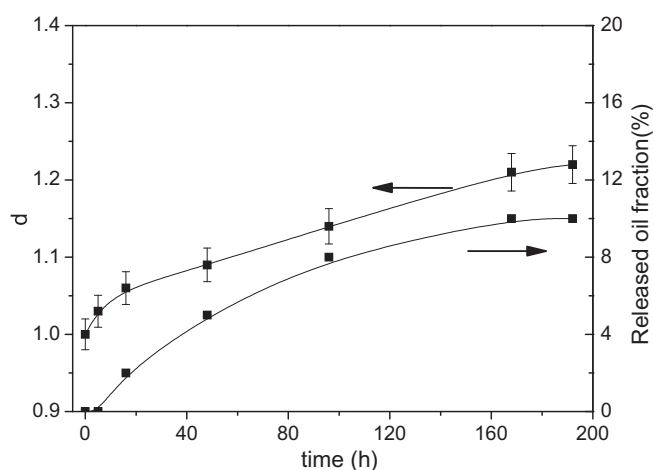


Fig. 4. Non-spherical degree of droplets (a) and releasing oil fraction of emulsion; (b) as a function of aging time at 80 °C with particle concentration of 0.29 wt.% and oil volume/total volume is 20%.

It is recognized that over the whole range of oil phase content, aging temperature and water/oil ratio closely links to the non-spherical degree of droplets. Based on the results above, the optimal conditions for the formation of non-spherical droplets are oil volume/total volume of 10–30% and temperature of 160–200 °C.

Aging time also is considered to be an important factor in the non-spherical process. As shown in Fig. 4, droplet fusion degree varied with aging time, while aging temperature and particle concentration remained constant at 80 °C and 0.29 wt.% respectively. When aging time was below 16 h, the d increased remarkably while the releasing oil fraction almost kept zero, indicating that the emulsion still stays stable macroscopically. But further increase of aging time would only see a slow increase of the d which means that aging time played a positive role in the formation of non-spherical droplets. Adequate aging time can ensure sufficient droplet contact and reasons for this would be discussed later.

From the optical micrographs of emulsions, we can find that at the aging temperature of 25 °C droplets remain spherical. Along with the rise of aging temperature, droplets present partial coalescence; several typical shapes are shown in Fig. 5 above. One droplet could fuse with another to form peanut shape, three neighboring droplets could fuse together to form rod-like shape. Four droplets or more could fuse to form some kind of irregular shape.

When the droplets fused by one droplet reach a certain number, not only the size and shape of the newly-formed droplet would change; but more importantly, the particle layer of it would become unstable, when the instability goes to its limit the particle layer would break up and thereby the oil phase inside would be released.

Generally, it is recognized that normal shearing action can hardly make the emulsion droplets fused because firm particle layer covering droplet surface has strong ability to resist coalescence [33]. Based on the results, it is inferred that there is a close relationship between particle layer properties and non-spherical droplets. Presumably under certain aging temperature, vacancy holes would appear in particle layer which probably is the reason of partial coalescence.

We now have recognized that non-spherical droplets can be formed through partial coalescence. An interesting question would be asked that why vacancy holes would present in particle layer.

To prevent droplet coalescence, generally it is necessary to ensure full coverage on droplet surface, such a situation could be explained by a simple equation [34].

$$\text{Coverage} = \frac{A_{\text{part}}^{\text{cov}}}{A_{\text{oil}}} = \frac{1}{\pi} \cdot \left(\frac{W_{\text{part}}}{W_{\text{oil}}} \right) \cdot \left(\frac{\rho_{\text{oil}}}{\rho_{\text{part}}} \right) \cdot \left(\frac{R_{\text{oil}}}{R_{\text{part}}} \right)$$

where A is the area, W is the weight, ρ is the density and R is the radius. In order to calculate the weight of solid particles, assuming 100% coverage as a jammed interface is desired.

From the equation, it is known that particle weight, oil weight, oil phase density and particle density are constant. The only changeable parameter is particle diameter. If particle size increased while particle weight stays the same, the total area covered by particles would decrease. According to the equation, it is not difficult to deduce that the coverage ratio should be below full coverage if particle size increased. In this case, partial coalescence would reduce the vacancy area in the particle layer.

To obtain the information of particle size variation under hydrothermal process, TEM and XRD were employed to investigate the variation of particle size, shape and crystalline. In our experiments, MPs can be easily synthesized by wet chemical precipitation at room temperature (25 °C) and the fresh sediment of MPs was used in the hydrothermal process under different aging temperatures. The crystalline structures of the obtained MPs at different temperatures are shown in Fig. 7. All diffraction peaks of the XRD pattern can be easily indexed to a pure hexagonal phase of MPs which is in agreement with the reported data (JCPDS 7-239) and literature [35]. The strong and sharp peaks observed confirm the resulted product was all well crystallized. The increasing peak intensity

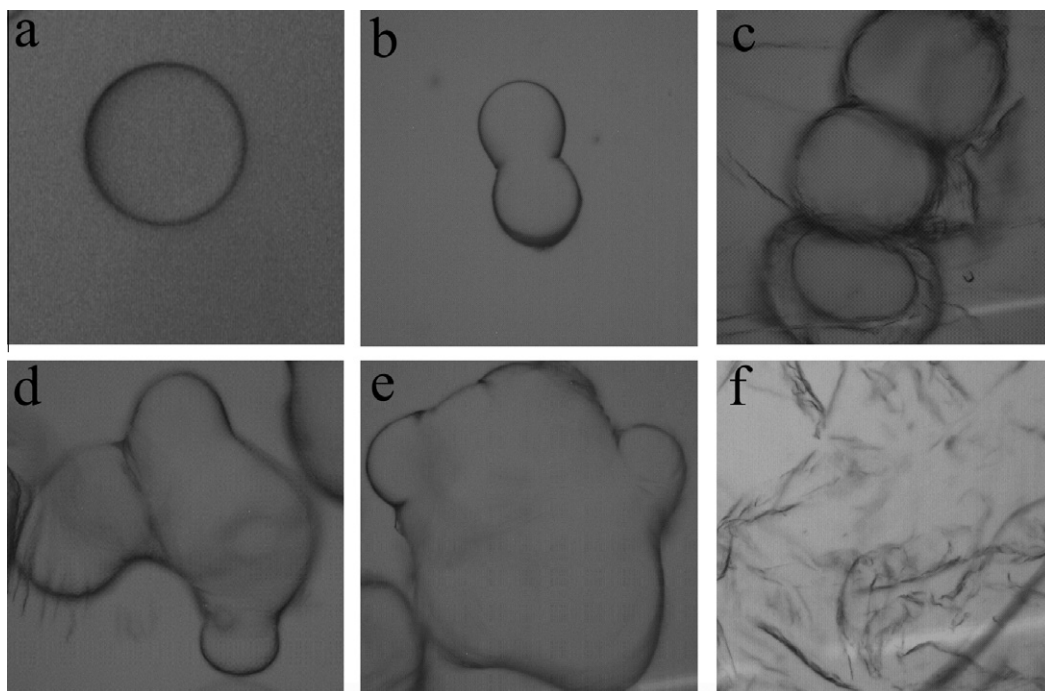


Fig. 5. Typical optical microphotographs of spherical droplets (a), non-spherical structures (b–e) and completely broken-up structures of particle layers (f).

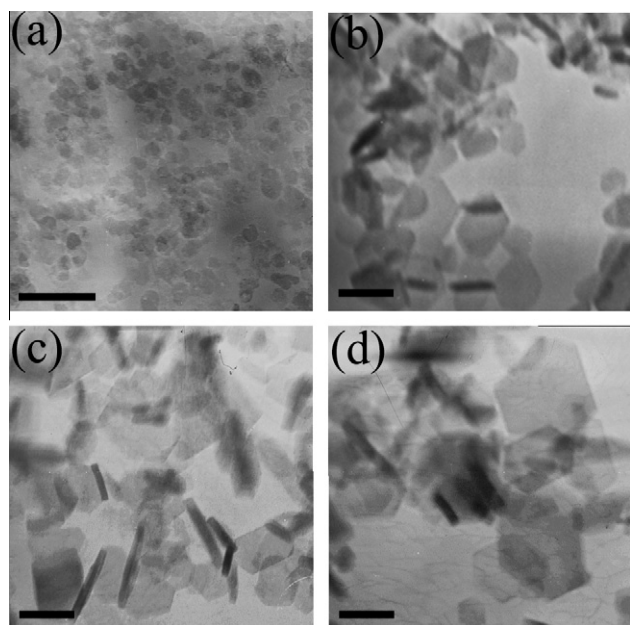


Fig. 6. TEM images of MPs were synthesized at 25 °C and then aged at: 25 (a), 80 (b), 120 (c), 200 °C (d) for 16 h. Scale bars in all images correspond to 100 nm.

with the rise of temperature indicates better crystalline and larger particle size. The morphology of MPs was visualized by TEM measurements. As shown in Fig. 6, the sample aged at the temperature of 25 °C consists of nanoplates with lateral dimension of 20–50 nm. With the rise of aging temperature, average size of particles increases from 80 nm at the aging temperature of 80 °C to 150 nm at the aging temperature of 200 °C. Moreover, it can be seen from the figure that MPs thickness is also increased along with the rise of aging temperature. The change of particle size in the TEM images is consistent with the results of XRD. From the equation above it is deduced that if the total weight stays the same while

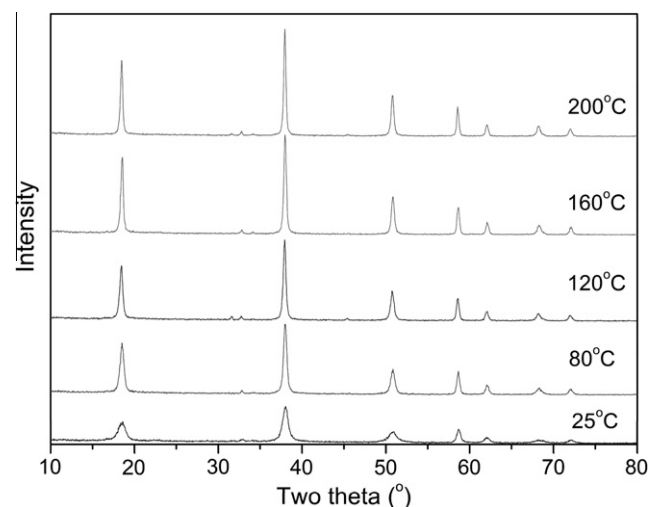


Fig. 7. XRD data of MPs were synthesized at 25 °C and then aged at different temperatures for 16 h.

the particle size increases, the total covering area would definitely decrease. In the hydrothermal process, the increase of particle size would be dominated by Ostwald ripening [35], namely, as the solubility of particles depends on their sizes under particular temperature, small particles would be dissolved while the large ones continue to grow.

Because of the increase of particle size, the total particle cover area decreases and vacant holes in the particle layer would show up, and these factors are the most important origins of fusion.

For emulsions stabilized by colloidal particles, a common phenomenon is that emulsion droplet size is strongly influenced by particle concentration within a certain range. Further increase of particle concentration after plateau values would not affect emulsion droplet size at all [36]. It can be seen from Fig. 8 that the drop

size keeps being reduced with the increase of particle concentration until a critical value is reached. Beyond this critical value excess particles appear. The excess particles were confirmed by the presence of a small shoulder of approximately 100 μm in the drop size distribution. For the fusion process, when the particle concentration was comparatively low, almost all the particles in the aqueous phase participated in the formation of particle layer at oil–water interface and there were hardly any particles left. In this case, partial coalescence between emulsion droplets could occur because of the vacant holes at high temperature. As during this process the particles increased were primarily used to cover more oil–water interface, the particles on the interface were mainly monolayer or multilayer and vacant holes in particle layer would appear after aging process. Partial coalescence would happen once these droplets collided and vacant holes in particle layer would be avoided. In the follow-up stage, the situation became more complicated [37]. The excess particles, on the one hand, may fix the vacancy holes in particle layer. On the other hand, it can cushion the collision between droplets. Moreover, if the aggregates or cluster of particles, which can be easily formed at high particle concentration, were absorbed on the droplet surfaces, they can also block the droplets from approaching, acting as a significant factor to prevent partial coalescence. Fig. 9 confirmed the two stages of stabilization of emulsions. At relatively low particle concentration, most

emulsion droplets present a circular particle layer, indicating that on the emulsion droplet surface, most particles are adsorbed on the interface in the form of single particle or small aggregates. But at relatively high particle concentrations, particles may form large aggregates.

To illustrate visually the structure of non-spherical droplet, SEM was employed to observe both the whole morphology and the surface. We tried to imitate this situation with polymerizable monomer instead of liquid paraffin. Monomer of styrene was used as oil phase and emulsions were kept at 160 °C and 200 °C separately. The styrene molecules could be polymerized in the absence of polymerization initiator, when the aging temperature was above 160 °C. From the images of SEM, it is recognized that non-spherical colloidal particles in Fig. 10a were resulted from fusing two spherical droplets while the ones in Fig. 10b were resulted from fusing four spherical droplets, and also it can be clearly seen that the fusing droplets were surrounded by plate-like particles with size of 150 nm and 200 nm. These phenomena again clearly demonstrated that non-spherical droplets can be formed through fusing the neighboring droplets. Based on the results above, it can be inferred that this approach could be applied to produce large quantities of non-spherical colloid particles, which are very important building blocks in the fabrication of complex nanostructured and microstructured materials [38,39]. Furthermore, if two or more mono-

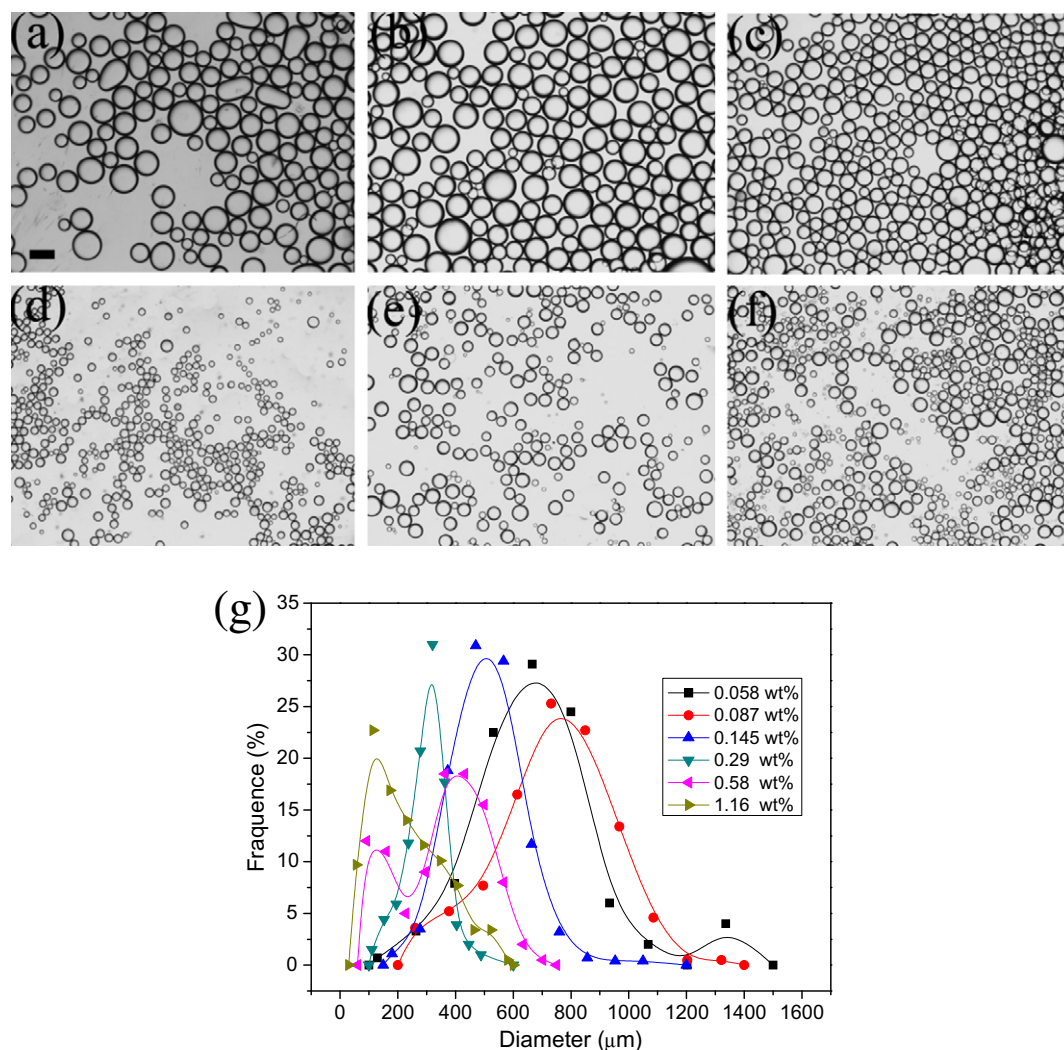


Fig. 8. Optical microscope images and size distribution of emulsion droplets prepared at different concentrations (oil/water = 1:1). The particle concentrations are: 0.058 (a), 0.087 (b), 0.145 (c), 0.29 (d), 0.58 (e), 1.16 (f) wt%. The data were measured after 48 h.

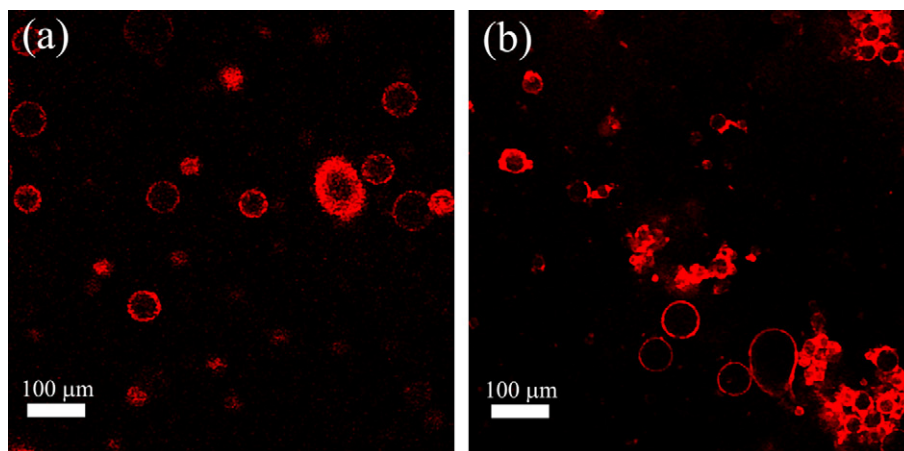


Fig. 9. Confocal fluorescence microscope images of emulsions at different particle concentrations: (a) 0.145 wt.% and (b) 1.16 wt.%.

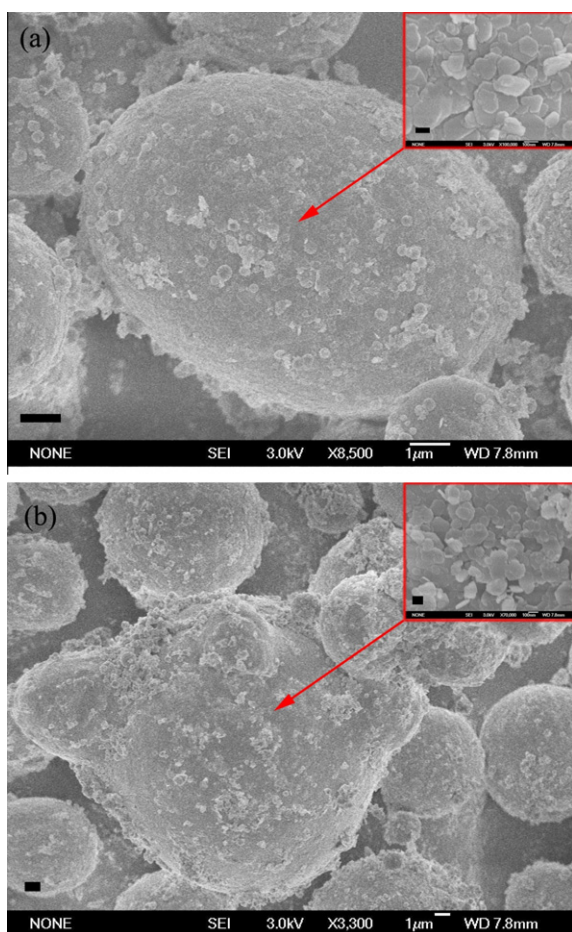


Fig. 10. Dried non-spherical structures formed by polymerizing the inner oil phase of droplets at the aging temperature of 160 °C (a) and 200 °C (b). Scale bars in all images correspond to 1 μm and inner images 100 nm.

mers with different wetting properties were used as oil phase, we may easily fabricate colloid particles with several different polarity heads, just like Janus particles [40–43].

On the whole, it is recognized that for non-spherical droplet production, three steps are required. Firstly, stable spherical droplets should be prepared by homogenizing oil/water mixture in the presence of surface – active particles. Secondly, the emulsion

should be kept at specific temperature to create particle vacant holes in droplet surface. Last, partial coalescence between the droplets nearby would occur and stable non-spherical droplets are produced. In addition, a very interesting case should be mentioned that in the To Ngai's work [44], emulsions stabilized by pH and temperature sensitive microgel particles underwent a similar temperature changing process. Microgel particles decreased their hydrodynamic size at a higher temperature and particle vacant holes in the droplet surface were clarified by SEM measurement. However, non-spherical droplets were not observed in his emulsion system, instead, droplet size increase was observed, presumably, this is either because it is much easier for such soft particles to adjust their position in the oil/water interface than for inorganic particles or because the particle layer composed of microgels is less rigid than that composed of inorganic particles. So far, the mechanism of non-spherical droplet formation has been demonstrated. The presence of non-spherical droplets is attributed to the intermediate situation between stable spherical droplets and complete coalescence. Though stable non-spherical droplets could easily be prepared by this method, precise control of partial coalescence is a limitation of this study. We expect that further research on tuning fusion would make up this limitation.

4. Conclusion

In summary, we have shown that non-spherical emulsion droplets can be produced by varying aging temperature. The non-spherical degree would be affected by aging temperature, particle concentration, and oil/water ratio and aging time. High temperature, relatively low oil/water ratio, intermediate particle concentration and long aging time would facilitate the formation of non-spherical droplets. All these factors have close link with the particle coverage of droplets and the excess particles on the interface. Based on the regulation of particle coverage on droplet surface, here we not only provide an approach to generate non-spherical droplets in large quantities but also offer some information about what would happen to particle coated droplets when particle coverage decreased on the droplet surface.

Acknowledgments

This work was financially supported by a grant from the Key Project of Chinese National Programs for Fundamental Research and Development (973 Program, No. 2009CB930100). The authors thank Ms. Yuying Lian for help in preparation of the manuscript.

References

- [1] Y.N. Xia, B. Gates, Y.D. Yin, Y. Lu, *Adv. Mater.* 12 (2000) 693.
- [2] L.S. Li, J.T. Hu, W.D. Yang, A.P. Alivisatos, *Nano Lett.* 1 (2001) 349.
- [3] M. Mittal, E.M. Furst, *Adv. Funct. Mater.* 19 (2009) 3271.
- [4] B. Madivala, J. Franssaer, J. Vermant, *Langmuir* 25 (2009) 2718.
- [5] J.C. Loudet, A.G. Yodh, B. Pouligny, *Phys. Rev. Lett.* (2006) 97.
- [6] E.P. Lewandowski, J.A. Bernate, A. Tseng, P.C. Searson, K.J. Stebe, *Soft Mater.* 5 (2009) 886.
- [7] W.Z. Zhou, J. Cao, W.C. Liu, S. Stoyanov, *Chem. – Int. Ed.* 48 (2009) 378.
- [8] S.H. Kim, G.R. Yi, K.H. Kim, S.M. Yang, *Langmuir* 24 (2008) 2365.
- [9] H.R. Sheu, M.S. El-Aasser, J.W. Vanderhoff, *J. Polym. Sci., Part A: Polym. Chem.* 28 (1990) 629.
- [10] E.B. Mock, H. De Bruyn, B.S. Hawkett, R.G. Gilbert, C.F. Zukoski, *Langmuir* 22 (2006) 4037.
- [11] C.C. Ho, A. Keller, J.A. Odell, R.H. Ottewill, *Polym. Sci.* 271 (1993) 469.
- [12] K. Zhao, C. Harrison, D. Huse, W.B. Russel, P.M. Chaikin, *Phys. Rev. E* (2007) 76.
- [13] O. Cayre, V.N. Paunov, O.D. Velev, *Mater. Chem.* 13 (2003) 2445.
- [14] A.R. Studart, H.C. Shum, D.A. Weitz, *Phys. Chem. B* 113 (2009) 3914.
- [15] S.A.F. Bon, S.D. Mookhoek, P.J. Colver, H.R. Fischer, S. van der Zwaag, *Eur. Polym. J.* 43 (2007) 4839.
- [16] A.B. Subramaniam, M. Abkarian, L. Mahadevan, H.A. Stone, *Nature* 438 (2005) 930.
- [17] S.C. Glotzer, M.J. Solomon, *Nat. Mater.* 6 (2007) 557.
- [18] T.L. Breen, J. Tien, S.R.J. Oliver, T. Hadzic, G.M. Whitesides, *Science* 284 (1999) 948.
- [19] S. Gangwal, O.J. Cayre, O.D. Velev, *Langmuir* 24 (2008) 13312.
- [20] R. Aveyard, B.P. Binks, J.H. Clint, *Adv. Colloid Interface Sci.* 100 (2003) 503.
- [21] F. Leal-Calderon, V. Schmitt, *Curr. Opin. Colloid Interface Sci.* 13 (2008) 217.
- [22] B.J. Park, E.M. Furst, *Langmuir* 26 (2010) 10406.
- [23] D. Lee, D.A. Weitz, *Small* 5 (2009) 1932.
- [24] Y.I. Dikanskii, O.A. Nechaeva, A.R. Zakinyan, *Colloid J.* 68 (2006) 137.
- [25] B. Walther, L. Hamberg, P. Walkenstrom, A.M. Hermansson, *Colloid Interface Sci.* 270 (2004) 195.
- [26] T. Sugimoto, M.M. Khan, A. Muramatsu, H. Itoh, *Colloids Surf., A* 79 (1993) 233.
- [27] C.C. Ho, A. Keller, J.A. Odell, R.H. Ottewill, *Colloid Polym. Sci.* 271 (1993) 469.
- [28] K.M. Keville, E.J. Franses, J.M. Caruthers, *Colloid Interface Sci.* 144 (1991) 103.
- [29] H.R. Sheu, M.S. El-Aasser, J.W. Vanderhoff, *J. Polym. Sci., Part A: Polym. Chem.* 28 (1990) 653.
- [30] A.T. Skjeltorp, J. Ugelstad, T. Ellingsen, *Colloid Interface Sci.* 113 (1986) 577.
- [31] J.J. Tan, J. Wang, L.Y. Wang, J. Xu, D.J. Sun, *J. Colloid Interface Sci.* 359 (2011) 155.
- [32] L. Desgranges, G. Calvarin, G. Chevrier, *Acta Crystallogr. Sect. B* 52 (1996) 82.
- [33] S. Arditty, C.P. Whitby, B.P. Binks, V. Schmitt, F. Leal-Calderon, *Eur. Phys. J. E* 11 (2003) 273.
- [34] S. Cauvin, P.J. Colver, S.A.F. Bon, *Macromolecules* 38 (2005) 7887.
- [35] J.C. Yu, A.W. Xu, L.Z. Zhang, R.Q. Song, L. Wu, *Phys. Chem. B* 108 (2004) 64.
- [36] B.P. Binks, S.O. Lumsdon, *Langmuir* 16 (2000) 2539.
- [37] B.P. Binks, *Curr. Opin. Colloid Interface Sci.* 7 (2002) 21.
- [38] Y.D. Yin, Y. Lu, Y.N. Xia, *Abstracts of Papers of the American Chemical Society*, vol. 221, 2001, p. 314.
- [39] Y. Lu, Y.D. Yin, Y.N. Xia, *Abstracts of Papers of the American Chemical Society*, vol. 22,1 2001, 170.
- [40] A. Perro, S. Reculosa, S. Ravaine, E.B. Bourgeat-Lami, E. Duguet, *Mater. Chem.* 15 (2005) 3745.
- [41] T. Nisisako, T. Torii, T. Takahashi, Y. Takizawa, *Adv. Mater.* 18 (2006) 1152.
- [42] K.H. Roh, D.C. Martin, J. Lahann, *Nat. Mater.* 4 (2005) 759.
- [43] A. Walther, A.H.E. Muller, *Soft Mater.* 4 (2008) 663.
- [44] T. Ngai, S.H. Behrens, H. Auweter, *Chem. Commun.* (2005) 331.